



1 **Introduction to the French GEOTRACES North Atlantic Transect**
2 **(GA01): GEOVIDE cruise**

3

4 Sarthou Géraldine ¹, Lherminer Pascale ², Achterberg Eric P. ³, Alonso-Pérez Fernando ⁴,
5 Bucciarelli Eva ¹, Boutorh Julia ¹, Bouvier Vincent ⁵, Boyle Edward A. ⁶, Branellec Pierre ²,
6 Carracedo Lidia I. ⁴, Casacuberta Nuria ⁷, Castrillejo Maxi ^{7,8}, Cheize Marie ^{1,9}, Contreira Pereira
7 Leonardo ¹⁰, Cossa Daniel ¹¹, Daniault Nathalie ², De Saint-Léger Emmanuel ¹², Dehairs Frank ¹³,
8 Deng Feifei ¹⁴, Desprez de Gésincourt Floriane ^{1,2}, Devesa Jérémy ¹, Foliot Lorna ¹⁵, Fonseca-
9 Batista Debany ^{13,16}, Gallinari Morgane ¹, García-Ibáñez Maribel I. ^{4,17}, Gourain Arthur ^{1,18},
10 Grossteffan Emilie ¹⁹, Hamon Michel ², Heimbürger Lars Eric ²⁰, Henderson Gideon M. ¹⁴,
11 Jeandel Catherine ⁵, Kermabon Catherine ², Lacan François ⁵, Le Bot Philippe ², Le Goff Manon
12 ¹, Le Roy Emilie ⁵, Lefèbvre Alison ², Leizour Stéphane ², Lemaitre Nolwenn ^{1,7,13}, Masqué Pere
13 ^{8,21}, Ménage Olivier ², Menzel Barraqueta Jan-Lukas ³, Mercier Herlé ², Perault Fabien ¹², Pérez
14 Fiz F. ⁴, Planquette Hélène F. ¹, Planchon Frédéric ¹, Roukaerts Arnout ¹², Sanial Virginie ^{5,22},
15 Sauzède Raphaëlle ²³, Shelley Rachel U. ^{1, 24}, Stewart Gillian ^{25,26}, Sutton Jill N. ¹, Tang Yi ^{26,25},
16 Tisnérat-Laborde Nadine ¹⁵, Tonnard Manon ^{1,27,28}, Tréguer Paul ¹, van Beek Pieter ⁵, Zurbrick
17 Cheryl M. ⁶, Zunino Patricia ²

18

19 1 CNRS, Univ. Brest, IRD, Ifremer, LEMAR (Laboratoire des Sciences de l'environnement
20 marin), Technopôle Brest-Iroise, 29280 Plouzané, France

21 2 Ifremer, Univ. Brest, CNRS, IRD, Laboratoire d'Océanographie Physique et Spatiale (LOPS),
22 IUEM, Plouzané, France

23 3 GEOMAR Helmholtz Centre for Ocean Research Kiel, 24124 Kiel, Germany

24 4 Instituto de Investigaciones Marinas, IIM-CSIC, Eduardo Cabello 6, 36208 Vigo, Spain

25 5 LEGOS (Laboratoire d'Etudes en Géophysique et Océanographie Spatiales), Université de
26 Toulouse, CNRS, CNES, IRD, UPS, 14 Avenue Edouard Belin, 31400 Toulouse, France

27 6 Earth, Atmospheric and Planetary Sciences, Massachusetts Institute of Technology,
28 Cambridge, MA 02139, USA

29 7 Laboratory of Ion Beam Physics, Department of Earth Sciences, Institute of Geochemistry
30 and Petrology, ETH-Zurich, Otto Stern Weg 5, Zurich, 8093, Switzerland

31 8 Institut de Ciència i Tecnologia Ambientals & Departament de Física, Universitat Autònoma
32 de Barcelona, Bellaterra, 08193, Spain

33 9 *Currently at* Laboratoire des cycles géochimiques, Géosciences Marines, Centre Ifremer
34 Bretagne

35 10 Laboratório de Hidroquímica-IO/FURG, Rio Grande, Brazil



- 36 11 ISTERre, Université Grenoble Alpes, CS 40700, 38058 GRENOBLE Cedex 9, France
- 37 12 CNRS, INSU, Division Technique Bâtiment IPEV - Centre Ifremer, Technopôle Brest-Iroise,
- 38 CS 50074, 29280 Plouzané, France
- 39 13 Analytical, Environmental and Geo-Chemistry, Vrije Universiteit Brussel, Pleinlaan 2, 1050,
- 40 Brussels, Belgium
- 41 14 Department of Earth Sciences, University of Oxford, South Parks Road, Oxford OX13AN, UK
- 42 15 LSCE/IPSL--CEA-CNRS-UVSQ--Université Paris Saclay, F-91198 Cedex, France
- 43 16 Department of Biology, Dalhousie University, Halifax, Nova Scotia B3H 4R2, Canada
- 44 17 Uni Research Climate, Bjerknes Centre for Climate Research, Bergen 5008, Norway
- 45 18 Ocean Sciences Department, School of Environmental Sciences, University of Liverpool,
- 46 Liverpool, 11 L69 3GP, UK
- 47 19 IUEM, UMS 3113, CNRS, Univ. Brest, IRD, Ifremer, Technopôle Brest Iroise, rue Dumont
- 48 d'Urville, 29280 PLOUZANE
- 49 20 Aix Marseille Université, CNRS/INSU, Université de Toulon, IRD, Mediterranean Institute of
- 50 Oceanography UM 110, Marseille, France
- 51 21 School of Science, Centre for Marine Ecosystems Research, Edith Cowan University,
- 52 Joondalup, WA 6027, Australia
- 53 22 *Currently at* Division of Marine Science, University of Southern Mississippi, 1020 Balch Blvd.
- 54 Stennis Space Center, MS 39529, USA
- 55 23 Sorbonne Universités, UPMC Univ Paris 06, CNRS, Laboratoire d'Océanographie de
- 56 Villefranche (LOV), 06230 Villefranche-sur-Mer, France
- 57 24 *Currently at* Earth, Ocean and Atmospheric Science, Florida State University, Tallahassee,
- 58 Florida 32306, USA
- 59 25 School of Earth and Environmental Sciences, Queens College, City University of New York,
- 60 Flushing, USA
- 61 26 Earth and Environmental Sciences, the Graduate Center, City University of New York, New
- 62 York, USA
- 63 27 Antarctic Climate and Ecosystem Cooperative Research Centre (ACE CRC), University of
- 64 Tasmania, Private Bag 80, Hobart, TAS 7001, Australia
- 65 28 Institute for Marine and Antarctic Studies, University of Tasmania, Hobart, TAS 7001,
- 66 Australia
- 67



68

69

70 **Abstract**

71 The GEOVIDE cruise, a collaborative project within the framework of the international
72 GEOTRACES programme, was conducted along the French-led section in the North Atlantic
73 Ocean (Section GA01), between 15 May and 30 June 2014. In this Special Issue, results from
74 GEOVIDE, including physical oceanography and trace element and isotope cyclings, are
75 presented among seventeen articles. Here, the scientific context, project objectives and
76 scientific strategy of GEOVIDE are provided, along with an overview of the main results from
77 the articles published in the special issue.

78

79

80 **1. Scientific context and objectives**

81

82 Understanding the distribution, sources, and sinks of trace elements and isotopes (TEIs) will
83 improve our ability to understand the past and present marine environments. Some TEIs are
84 toxic (e.g. Hg), while others are essential micronutrients involved in many metabolic processes
85 of marine organisms (e.g. Fe, Mn). The availability of TEIs therefore constrains the ocean
86 carbon cycle and affects a range of other biogeochemical processes in the Earth system, whilst
87 responding to and influencing global change (de Baar et al., 2005; Blain et al., 2007; Boyd et
88 al., 2007; Pollard et al., 2007). Moreover, TEI interactions with the marine food web strongly
89 depend on their physical (particulate/dissolved/colloidal/soluble) and chemical (organic and
90 redox) forms. In addition, some TEIs are diagnostic in allowing the quantification of specific
91 mechanisms in the marine environment that are challenging to measure directly. A few
92 examples include: (i) atmospheric deposition (e.g. ^{210}Pb , Al, Mn, Th isotopes, ^7Be ; Baker et al.,
93 2016; Hsieh et al., 2011; Measures and Brown, 1996), (ii) mixing rates of deep waters or shelf-
94 to-open ocean (e.g. $^{231}\text{Pa}/^{230}\text{Th}$, $\delta^{14}\text{C}$, Ra isotopes, ^{129}I , ^{236}U ; van Beek et al., 2008; Casacuberta
95 et al., 2016; Key et al., 2004), (iii) boundary exchange processes (e.g. ϵ_{Nd} , Jeandel et al., 2011;
96 Lacan and Jeandel, 2001, 2005), and (iv) downward flux of organic carbon and/or
97 remineralisation in deep waters (e.g. $^{234}\text{Th}/^{238}\text{U}$, $^{210}\text{Pb}/^{210}\text{Po}$, Ba_{xs} ; Buesseler et al., 2004;
98 Dehairs et al., 1997; Roca-Martí et al., 2016). In such settings, TEIs provide chemical
99 constraints and allow the estimation of fluxes which was not possible before the development



100 of their analyses. Finally, paleoceanographers are wholly dependent on the development of
101 tracers, many of which are based on TEIs used as proxies, in order to reconstruct past
102 environmental conditions (e.g. ocean productivity, patterns and rates of ocean circulation,
103 ecosystem structures, ocean anoxia; Henderson, 2002). Such reconstruction efforts are
104 essential to assess the processes involved in regulating the global climate system, and possible
105 future climate change variability.

106 Despite all these major implications, the distribution, sources, sinks, and internal cycling of
107 TEIs in the oceans are still largely unknown due to the lack of appropriate clean sampling
108 approaches and insufficient sensitivity and selectivity of the analytical measurement
109 techniques until recently. This last point has improved very quickly as significant
110 improvements in the instrumental techniques now allow the measurements of
111 concentrations, speciation (physical and chemical forms), and isotopic compositions for most
112 of the elements of the periodic table which have been identified either as relevant tracers or
113 key nutrients in the marine environment. These recent advances provide the marine
114 geochemistry community with a significant opportunity to make substantial contributions to
115 a better understanding of the marine environment.

116

117 In this general context, the aim of the international GEOTRACES programme is to
118 characterize TEI distributions on a global scale, consisting of ocean sections, and regional
119 process studies, using a multi-proxy approach. The GEOVIDE section is the French contribution
120 to this global survey in the North Atlantic Ocean along the OVIDE section and in the Labrador
121 Sea (Fig. 1) and complements a range of other international cruises in the North Atlantic.
122 GEOVIDE leans on the knowledge gained by the OVIDE project during which the Portugal-
123 Greenland section has been carried out biennially since 2002, gathering physical and
124 biogeochemical data from surface to bottom (Mercier et al., 2015; Perez et al., 2018).

125

126

127 Rationale for the GEOVIDE section:

128 i) The North Atlantic Ocean plays a key role in mediating the climate of the Earth. It
129 represents a key region of the Meridional Overturning Circulation (MOC) and a major sink of
130 anthropogenic carbon (C_{ant}) (Pérez et al., 2013; Sabine et al., 2004; Seager et al., 2002). Since
131 2002, the OVIDE project has contributed to the observation of both the circulation and water



132 mass properties of the North Atlantic Ocean. Despite the importance of the MOC on global
133 climate, it is still challenging to assess its strength within a reasonable uncertainty (Kanzow et
134 al., 2010; Lherminier et al., 2010). The MOC strength estimated from *in-situ* measurements on
135 OVIDE cruises has thus helped to validate a time series for the amplitude of the MOC (based
136 on altimetry and ARGO float array data) that exhibits a drop of 2.5 ± 1.4 Sv (95% confidence
137 interval) between 1993 and 2010 (Mercier et al., 2015), consistent with other modelling
138 studies (Xu et al., 2013). This time series, along with the *in situ* data, shows a recovery of the
139 MOC amplitude in 2014 at a value similar to those of the mid-1990s, confirming the
140 importance of the decadal variability in the subpolar gyre. During OVIDE, the contribution of
141 the most relevant currents, water masses and biogeochemical provinces have been localized
142 and quantified. This knowledge was crucial for the establishment of the best strategy to
143 sample TEIs in this specific region.

144 In addition to the OVIDE section, the Labrador Sea section offered a unique opportunity to
145 complement the MOC estimate, to analyse the propagation of anomalies in temperature and
146 salinity (Reverdin et al., 1994), and to study the distribution of TEIs along the boundary current
147 of the subpolar gyre, coupling both observations and modelling.

148 Moreover, recent results provided evidences that CO_2 uptake in the North Atlantic was
149 reduced by the weakening of the MOC (Pérez et al., 2013). The most significant finding of this
150 study was that the uptake of C_{ant} occurred almost exclusively in the subtropical gyre, while
151 natural CO_2 uptake dominated in the subpolar gyre. In light of these new results, one issue to
152 be addressed was the coupling between the C_{ant} and the transport of water, with the aim to
153 understand how the changes in the ventilation and in the circulation of water masses affect
154 the C_{ant} uptake and its storage capacity in the various identified provinces (Fröb et al., 2018).

155 Finally, as the subpolar North Atlantic forms the starting point for the global ocean conveyor
156 belt, it is of particular interest to investigate how TEIs are transferred to the deep ocean
157 through both ventilation and particle sinking, and how deep convection processes impact the
158 TEI distributions in this key region.

159

160 ii) A better assessment of the factors that control organic production and export of carbon
161 in the productive North Atlantic Ocean, together with a better understanding of the role
162 played by TEIs in these processes are research priorities. Pronounced phytoplankton blooms
163 occur in the North Atlantic in spring in response to upwelling and water column



164 destratification (Bury et al., 2001; Henson et al., 2009; Savidge et al., 1995). Such blooms are
165 known to trigger substantial export of fast-sinking particles (Lampitt, 1985), and can represent
166 a major removal mechanism for particulate organic carbon, macronutrients, and TEIs to the
167 deep ocean.

168

169 iii) In the North Atlantic, TEI distributions are influenced by a variety of sources including, for
170 the most important, the atmosphere and the margins (Iberian, Greenland, and Labrador
171 margins).

172

173 *Atmosphere:* Atmospheric inputs (e.g. mineral dust, anthropogenic emission aerosols) are an
174 important sources of TEIs to the North Atlantic Ocean due to the combined effects of
175 anthropogenic emissions from industrial/agricultural sources and mineral dust mobilized from
176 the arid regions of North Africa (Duce et al., 2008; Jickells et al., 2005). Model and satellite
177 data for the GEOVIDE section suggested that an approximately tenfold decrease in the
178 atmospheric concentrations of mineral dust was expected from south to north (Mahowald et
179 al., 2005). As there had been relatively few aerosol TEI studies in the northern North Atlantic
180 compared to the tropical and subtropical North Atlantic prior to GEOVIDE, constraining
181 atmospheric deposition fluxes to this region had been identified as a research priority (de
182 Leeuw et al., 2014). During the GEOVIDE campaign, a multi-proxy approach (e.g. aerosol trace
183 element concentrations, dissolved and particulate Al and Mn, seawater ²¹⁰Pb, Fe, Nd and Th
184 isotopes, ⁷Be) was taken to achieve the objective of better constraining the atmospheric
185 deposition fluxes of key trace elements.

186

187 *Margins:* The continental shelves can act as a filter for TEIs supplied from shelf sediments,
188 submarine groundwater discharge (including the discharge of fresh groundwater into the
189 coastal seas and recirculation of seawater through the sediment), and rivers. While some TEIs
190 are removed on the continental shelves, others are thought to be mobilized from the solid
191 phase at the land-ocean interface (e.g. Fe and likely other micro- and macro-nutrients, such
192 as Cu, Ni, Mn, and Si; Chase et al., 2005; Jeandel and Oelkers, 2015). The cruise track
193 intersected several margins, thus allowing for the characterization of continental sources and
194 quantification of TEIs fluxes associated with these sources in various shelf regimes.

195



196 iv) It is obviously needed to further validate the use of paleo-proxies. For example, in recent
197 years, the potential of the $^{231}\text{Pa}/^{230}\text{Th}$ ratio for identifying past rates of ocean circulation, and
198 of the isotopic composition of neodymium (ϵ_{Nd}) as a tracer of thermohaline circulation have
199 led to many paradigm-changing results for the reconstitution of the Atlantic Ocean circulation
200 (McManus et al., 2004; Montero-Serrano et al., 2013; Negre et al., 2010). However, there is
201 an ongoing debate about the interpretation of $^{231}\text{Pa}/^{230}\text{Th}$ paleo-records in the Atlantic (Hayes
202 et al., 2015; Keigwin and Boyle, 2008) focused on the effects of particle fluxes versus those of
203 water circulation. Only one single ^{231}Pa profile in the Subpolar North Atlantic has been
204 published before GEOVIDE (Moran et al., 2002). Regarding Nd isotopes, although several
205 profiles of dissolved (and total) Nd isotopes are available in the boundary currents of
206 Greenland and the Labrador Sea, there are very few profiles for the ocean interior of the
207 GEOVIDE region (Copard et al., 2011; Filippova et al., 2017; Lacan and Jeandel, 2004; Lambelet
208 et al., 2016). In addition, the importance of dissolved/particle interactions in the control of
209 the isotopic composition of Nd is becoming increasingly apparent. To our knowledge,
210 particulate ϵ_{Nd} data has not been published yet for the Subpolar North Atlantic. For these
211 reasons, documenting these tracers in both dissolved and particulate phases is needed to
212 provide new constraints and significantly advance our understanding of the cycles of these
213 tracers and their use in the modern and past oceans.

214 Furthermore, proxies of nutrient utilization, such as the silicon stable isotopes ($\delta^{30}\text{Si}$) from
215 diatom silica, provides a means of reconstructing the behaviour of past geochemical cycles
216 and the past strength of the biological pump, and its influence on atmospheric concentrations
217 of CO_2 . However, successful application of $\delta^{30}\text{Si}$ in diatoms accumulating in sediments for
218 reconstruction of past silica cycling requires a thorough understanding of $\delta^{30}\text{Si}$ of dissolved Si
219 (DSi) and of the processes that control its distribution throughout the modern ocean.
220 Combining studies in the Southern Ocean (De La Rocha et al., 2011; Fripiat et al., 2011) and
221 North and Equatorial Pacific (De La Rocha et al., 2000) with a global circulation model
222 (Wischmeyer et al., 2003) has revealed the roles that ocean circulation and biogeochemical
223 cycling play in controlling the distribution of silicon isotopes within the ocean. Largely missing
224 from this dataset was the North Atlantic Ocean (De La Rocha et al., 2011).

225

226 In this general context, the main scientific objectives of GEOVIDE were to (i) better
227 understand and quantify the MOC and the carbon cycle carbon cycle in the context of decadal



228 variability, adding new tracers to this end, (ii) map the TEI distributions, including their physical
229 and chemical speciation, along this full-depth high resolution ocean section, (iii) investigate
230 the links between TEIs and the production, export, and remineralisation of particulate organic
231 matter, (iv) identify TEI sources and sinks, and quantify their fluxes at the ocean boundaries,
232 and (v) better understand and quantify the paleoproxies $^{231}\text{Pa}/^{230}\text{Th}$, ϵ_{Nd} , and $\delta^{30}\text{Si}$.

233

234

235 2. Strategy

236

237 To achieve the objectives of the GEOVIDE project, a 47-day multidisciplinary cruise was
238 carried out on board R/V Pourquoi Pas? in the North Atlantic Ocean along the OVIDE section,
239 from Lisbon to Greenland, and in the Labrador Sea (Fig. 1). The Labrador section was chosen
240 according to the OSNAP (Overturning in the Subpolar North Atlantic Programme)
241 recommendations because it transects the export route of the Labrador Sea Water
242 downstream of its formation site. Therefore, the properties of the North Atlantic Deep Water
243 (NADW) at 53°N are likely to be representative of NADW further south and a 15-year time
244 series of currents and hydrographic properties is available in the Western Boundary Current
245 at this latitude (Fischer et al., 2010). The GEOVIDE cruise took place from 15 May to 30 June
246 2014, during the same season as the previous OVIDE cruises (2002-2012). The cruise timing
247 helped to minimize seasonal variations and maximize the representativeness of inter-annual
248 variability of the physical parameters investigated in this specific region. Furthermore, this
249 period of the year corresponds to the bloom/post-bloom period of the subpolar gyre and post-
250 bloom period in the sub-tropical gyre (Henson et al., 2005), thus allowing for the study of the
251 complexity of the biological pump and the links between production, export of organic matter,
252 and TEIs.

253 A high resolution hydrographical section that includes the *in-situ* measurements of the
254 currents by doppler profilers was performed and, as recommended by GEOTRACES, a multi-
255 proxy approach was used. In total, 78 stations were occupied (plus one test station). Station
256 naming depended on the number of casts that were conducted: Short (47 one-cast stations),
257 Large (17 three-cast stations), XLarge (5 five-cast stations), and Super (10 multi-cast stations).
258 A total of 341 on-deck operations were carried out during GEOVIDE.



259 In total, (i) the standard stainless steel rosette was deployed 163 times, (ii) the trace metal
260 clean rosette, 53 times, (iii) *in-situ* pumps, 25 times, (iv) the mono-corer, with or without *in-*
261 *situ* pumps clamped on the cable, 11 times and (v) the plankton net, 9 times. We also collected
262 140 surface seawater samples using a fish towed from the ship's starboard side and deployed
263 at 1–2 m depth, 18 aerosol samples, and 10 rainwater samples. In addition, we deployed: 60
264 expendable BathyThermographs (XBTs), 17 ARGO profiling floats (8 ARVOR, 2 ARVOR-deep, 2
265 PROVOR-DO, 2 PROVBIO, 1 ARVOR double DO, and 2 APEX), and 12 weather buoys.

266

267

268 3. Summary of the main results published in this special issue

269

270 In this special issue, seventeen publications present results of the GEOVIDE project. Six other
271 manuscripts have already been published in other journals (Benetti et al., 2017; Cossa et al.,
272 2018b; Le Reste et al., 2016; Perez et al., 2018; Shelley et al., 2017; Zunino et al., 2015). Due
273 to the long time required for some analyses, other articles related to this project are to be
274 expected for publication at a later date.

275 The articles in this special issue are linked to four general research themes: (i) hydrographic
276 and physical characteristics, (ii) links between water masses and TEIs, (iii) external sources and
277 sinks of TEIs, and (iv) biogeochemical tracers of community structure, export and
278 remineralisation.

279

280 3.1. Hydrographic and physical characteristics

281 In terms of circulation, the comparison with the 2002–2012 mean state shows a different
282 repartition of the northward warm currents that compose the upper limb of the MOC, with a
283 more intense Irminger Current (station 39–41) and a weaker North Atlantic Current in the
284 Western European Basin, these anomalies being compatible with the variability previously
285 observed along the OVIDE section in the 2000s (Zunino et al., 2017).

286 The main hydrographic properties along the GEOVIDE section are shown on Fig. 2 for
287 potential temperature, salinity, dissolved oxygen, nitrate + nitrite, and silicic acid. The surface
288 waters of the eastern SPNA, down to about 500 m, were much colder and fresher than the
289 average values observed over 2002–2012 (Zunino et al., 2017). In the context of the ocean
290 heat loss observed in the subpolar gyre since 2005, the year 2013–2014 was indeed particularly



291 intense. Remarkably, despite the negative temperature anomalies in the surface waters, the
292 heat transport across the OVIDE section estimated during GEOVIDE was the largest measured
293 since 2002 and attributed to the relatively strong MOC measured across the OVIDE section
294 during GEOVIDE (Zunino et al., 2017).

295 The water mass properties of the GEOVIDE cruise were used to perform an extended
296 Optimum MultiParameter (eOMP) analysis and to assess the water mass distribution (García-
297 Ibáñez et al., 2018). The eOMP analysis together with the absolute geostrophic velocity field
298 determined using a box inverse model allowed the evaluation of the relative importance of
299 each water mass to the MOC. The increase in the MOC intensity from 2002–2010 to 2014 was
300 shown to be related to the increase in the northward transport of the Central Waters in its
301 upper limb, and in the southward flow of Subpolar Mode Water (SPMW) of the Irminger Basin
302 and Iceland–Scotland Overflow Water (ISOW) in its lower limb (García-Ibáñez et al., 2018).

303 In addition, the precise determination of different water masses (García-Ibáñez et al., 2018)
304 and ventilation processes are crucial for the interpretation of the TEIs whose distributions are,
305 for many of them, strongly related to water masses.

306

307

308 3.2. Links between water masses and TEIs

309 The concentrations of TEIs are strongly influenced by water mass distribution, age, and
310 circulation/mixing. For instance, this is the case of ^{230}Th and ^{231}Pa , high concentrations of both
311 tracers were observed in the old water of North East Atlantic Deep Water (NEADW), and low
312 values in young waters, particularly in Denmark Strait Overflow Water (DSOW) (Deng et al.,
313 2018). The low values of ^{230}Th and ^{231}Pa in water near the seafloor of the Labrador and
314 Irminger Seas are related to the young waters present in those regions (Deng et al., 2018).
315 This study reports systematic increase of ^{230}Th activities with water age but a more complex
316 relationship between age and ^{231}Pa which challenges some approaches to the use of
317 sedimentary $^{231}\text{Pa}/^{230}\text{Th}$ ratios to assess past rates of oceanic circulation. The application of
318 this proxy at a basin scale to constrain the overturning circulation is, however, supported by
319 GEOVIDE data which now allows a complete nuclide budget for the North Atlantic to be
320 constructed (Deng et al., 2018).

321 Long-lived artificial radionuclides were also very useful to assess the circulation in the
322 SPNA, namely ^{129}I and ^{236}U , and the origin of water masses in a dual tracer approach (i.e.



323 $^{129}\text{I}/^{236}\text{U}$ and $^{236}\text{U}/^{238}\text{U}$ atom ratios) (Castrillejo et al., 2018). These transient tracers, originating
324 from La Hague (France) and Sellafield (UK) nuclear reprocessing plants and the atmospheric
325 nuclear weapon tests, helped investigating the shallow western boundary transport and the
326 ventilation processes. For example, the ^{129}I concentrations validate the ISOW transport
327 pathways in the Western European basin. The time series of ^{129}I in the Labrador Sea revealed
328 two circulation loops of the Atlantic Waters carrying the signal from the European
329 reprocessing plants: i) a short loop through the Nordic Seas into the central Labrador Sea of
330 about 8-10 years, and; ii) a longer loop which includes about 8 additional years of recirculation
331 in the Arctic Eurasian Basin before entering back to the Atlantic Ocean (Castrillejo et al., 2018).

332 Some other TEIs were also strongly linked to water mass distribution: Within GEOVIDE,
333 silicon isotopes (Sutton et al., 2018), lead (Pb) (Zurbrick et al., 2018), mercury (Hg) (Cossa et
334 al., 2018a), and particulate and dissolved Fe and Al (Gourain et al., 2018; Menzel Barraqueta
335 et al., 2018b; Tonnard et al., 2018), as examples. For instance, the Labrador Seawater (LSW) is
336 characterized by a relatively high silicon stable isotope composition for dissolved silicon
337 ($\delta^{30}\text{Si}_{\text{DSi}}$) whose signature can be seen not only in the region where it is formed, but also
338 throughout the mid-depth zone of the North Atlantic Ocean (Sutton et al., 2018). The $\delta^{30}\text{Si}_{\text{DSi}}$
339 distribution thus provides information on the interaction between subpolar/polar water
340 masses of northern and southern origin, and indicates the extent to which local signatures are
341 influenced by source waters (Sutton et al., 2018). In LSW, the concentrations of Pb (Zurbrick
342 et al., 2018) and Hg (Cossa et al., 2018a) provided evidence for a decrease in the
343 anthropogenic inputs of these two elements over the last decade, since the values are lower
344 in the recently formed LSW between Greenland and Newfoundland than in the older LSW of
345 the Western European basin.

346 The Mediterranean Water (MW), meanwhile, was characterised by higher concentrations
347 of trace metals, such as Pb, Hg, and Al (Cossa et al., 2018a; Menzel Barraqueta et al., 2018b;
348 Zurbrick et al., 2018). It reflects the importance of Saharan and anthropogenic atmospheric
349 inputs to the Mediterranean region, which are much higher than in our studied area (see
350 below), as well as enhanced remineralisation as indicated by the correlation between total
351 mercury concentrations and the apparent oxygen utilisation (Cossa et al., 2018a).

352

353

354



355 3.3. TEI sources and sinks

356 Different methods/TEIs were used to estimate atmospheric input fluxes: aerosol
357 concentrations in aerosol and rainwater samples were compared with estimates derived from
358 the measurement of beryllium-7 (^7Be) in aerosols, rainwater and seawater (Shelley et al.,
359 2017). Taking a different approach, Menzel Barraqueta et al. (2018a) used dAl in the surface
360 waters to estimate the atmospheric input flux. All these methods allowed concluding that the
361 atmospheric inputs of total trace elements were low in our study area, and the soluble input
362 was even lower, based on their fractional solubility (Shelley et al., 2018).

363 One of the main sources of TEIs during GEOVIDE was sediment input (i) within the benthic
364 nepheloid layers in the Iceland, Irminger and Labrador Basins, and (ii) above the Iberian,
365 Greenland and Canadian margins, as well as fluvial and meteoric inputs (Benetti et al., 2017).
366 This is notably the case for some dissolved TEIs, such as Fe (Tonnard et al., 2018), Al (Menzel
367 Barraqueta et al., 2018b), and radium-226 (^{226}Ra) or barium (Ba) (Le Roy et al., 2017), as well
368 as for particulate trace elements (Gourain et al., 2018). Overall, enhanced concentrations of
369 TEIs close to the bottom suggest that continental shelves and margins acted as a source to
370 adjacent waters. In the case of the Iberian margin, advection of particulate Fe (pFe) was visible
371 over a distance of more than 250 km from the source (Gourain et al., 2018).

372 However, some results provide evidence that occasional removal of dFe or dAl by particles
373 can be a dominant process rather than partial dissolution from resuspended sediments, but
374 this is likely dependent on the nature of particles (Menzel Barraqueta et al., 2018b).

375 Additional sources for particulate elements and sinks for dissolved ones are biological
376 uptake and scavenging. Evidence for a biogenic influence on the pFe/pAl ratios within the
377 Irminger and Labrador Basins was found by Gourain et al. (2018). Almost all the stations
378 displayed dFe minima in surface waters, in association with the chlorophyll maxima. The
379 abundance of diatoms exerted a significant control on the surface concentrations of Fe and Al
380 (Menzel Barraqueta et al., 2018a; Tonnard et al., 2018). Remineralisation processes were also
381 highlighted for some TEIs (see also section 3.4). Dissolved Al concentrations generally
382 increased with depth and the net release of dAl at depth during remineralisation of sinking
383 biogenic opal containing particles was generally larger than the net removal of dAl through
384 scavenging.

385

386



387 3.4. Production, export, and remineralisation

388 The main biogeochemical features of the GEOVIDE cruise in terms of biogenic silica (BSi),
389 particulate organic carbon (POC), and particulate organic nitrogen (PON) are reported on Fig.
390 3 and supplementary material. The higher BSi concentrations were observed in the Irminger
391 and Labrador Seas. POC and PON were also high in these regions, but also show high values in
392 the Iceland and Western European Basins.

393 On the Iberian margin and in the Western European Basin, an unexpectedly high
394 heterotrophic nitrogen fixation activity was reported, likely sustained by the availability of
395 phytoplankton-derived organic matter (dissolved and/or particulate), resulting from the on-
396 going to post spring bloom conditions, while dissolved iron supply relied on atmospheric
397 deposition and surface waters advection from the subtropical region and the shelf area
398 (Fonseca-Batista et al., 2018).

399 In terms of particulate organic carbon (POC) export, thorium-234 (^{234}Th) was used to
400 provide estimates of POC export fluxes, with the highest values near the Iberian margin where
401 a phytoplankton bloom was declining, and the lowest values in the Irminger Basin where the
402 bloom was close to its maximum (Lemaitre et al., 2018a). The proxy $^{210}\text{Po}/^{210}\text{Pb}$ was also used
403 to assess the export of particles (Tang et al., 2018). The prominent role of small particles in
404 sorption was confirmed, suggesting that particulate radionuclide activities and export of both
405 small (1-53 μm) and large (> 53 μm) particles should be considered to account for the observed
406 surface water $^{210}\text{Po}/^{210}\text{Pb}$ disequilibria (Tang et al., 2018).

407 In the subpolar and subtropical regions, the mesopelagic POC remineralisation fluxes,
408 estimated from the particulate biogenic barium (excess barium; Ba_{xs}) proxy, were found to be
409 equal to and occasionally higher than the upper ocean POC export fluxes (Lemaitre et al.,
410 2018b). These results highlighted the strong impact of the mesopelagic remineralisation on
411 the biological carbon pump with a very low carbon sequestration efficiency at the time of our
412 study (Lemaitre et al., 2018b).

413

414

415

416

417

418



419 **Conclusion**

420 The main GEOVIDE results have helped to improve our understanding of the TEI cycles in the
421 North Atlantic. The strong physical oceanography background of the GEOVIDE project is a
422 strength for interpreting our data. For many TEIs, a strong link was observed between their
423 distributions and water masses. On the other hand, TEIs also helped to constrain oceanic
424 circulation, notably in the subpolar gyre and Labrador Sea. Important sources (sediments,
425 fluvial, and meteoric) and sinks (biological uptake and scavenging) of TEIs were highlighted.
426 The biological carbon pump was studied and showed different efficiencies in the various
427 studied regions.

428

429

430 **Acknowledgements:**

431 We are greatly thankful to the captain, Gilles Ferrand, and crew of the N/O Pourquoi Pas?
432 for their help during the GEOVIDE mission. This work was supported by the French National
433 Research Agency (ANR-13-BS06-0014, ANR-12-PDOC-0025-01), the French National Centre for
434 Scientific Research (CNRS-LEFE-CYBER), the LabexMER (ANR-10-LABX-19), and Ifremer. It was
435 supported for the logistic by DT-INSU and GENAVIR.

436

437

438 **References**

- 439 de Baar, H. J. W., Boyd, P. X., Coale, K. H., Landry, M. R., Tsuda, A., Assmy, P., Bakker, D. C. E., Bozec,
440 Y., Barber, R. T., Brzezinski, M. A., Buesseler, K. O., Boye, M., Croot, P. L., Gervais, F., Gorbunov, M.
441 Y., Harrison, P. J., Hiscock, W. T., Laan, P., Lancelot, C., Law, C. S., Levasseur, M., Marchetti, A., Millero,
442 F., Nishioka, J., Nojiri, Y., van Oijen, T., Riebesell, U., Rijkenberg, M. J. A., Saito, H., Takeda, S.,
443 Timmermans, K. R., Veldhuis, M. J. W., Waite, A. M. and Wong, C.-S.: Synthesis of iron fertilization
444 experiments: From the Iron Age in the Age of Enlightenment, *J Geophys Res*, 110, C09S16,
445 doi:10.1029/2004JC002601, 2005.
- 446 Baker, A. R., Landing, W. F., Bucciarelli, E., Cheize, M., Fietz, S., Hayes, C. T., Kadko, D., Morton, P. L.,
447 Rogan, N., Sarthou, G., Shelley, R. U., Shi, Z., Shiller, A. M. and Van Hulten, M. M. P.: Air - Sea
448 Deposition of Trace Elements | Philosophical Transactions of the Royal Society of London A:
449 Mathematical, Physical and Engineering Sciences, [online] Available from:
450 <http://rsta.royalsocietypublishing.org/content/374/2081/20160190> (Accessed 18 June 2018), 2016.
- 451 van Beek, P., Bourquin, M., J.-L., R., Souhaut, M., Charette, M. A. and Jeandel, C.: Radium isotopes to
452 investigate the water mass pathways on the Kerguelen Plateau (Southern Ocean), *Deep Sea Res II*,
453 55(5–7), 622–637, 2008.
- 454 Benetti, M., Reverdin, G., Lique, C., Yashayaev, I., Holliday, N. P., Tynan, E., Torres-Valdes, S.,
455 Lherminier, P., Tréguer, P. and Sarthou, G.: Composition of freshwater in the spring of 2014 on the
456 southern Labrador shelf and slope, *J. Geophys. Res. Oceans*, 122(2), 1102–1121,
457 doi:10.1002/2016JC012244, 2017.
- 458 Blain, S., Quéguiner, B., Armand, L., Belviso, S., Bombled, B., Bopp, L., Bowie, A., Brunet, C., Brussaard,
459 C., Carlotti, F., Christaki, U., Corbière, A., Durand, I., Ebersbach, F., Fuda, J.-L., Garcia, N., Gerringa, L.,
460 Griffiths, B., Guigue, C., Guillermin, C., Jacquet, S., Jeandel, C., Laan, P., Lefèvre, D., Lomonaco, C.,
461 Malits, A., Mosseri, J., Obernosterer, I., Park, Y.-H., Picheral, M., Pondaven, P., Remenyi, T., Sandroni,
462 V., Sarthou, G., Savoye, N., Scouarnec, L., Souhaut, M., Thuiller, D., Timmermans, K., Trull, T., Uitz, J.,
463 van-Beek, P., Veldhuis, M., Vincent, D., Viollier, E., Vong, L. and Wagener, T.: Impact of natural iron
464 fertilization on carbon sequestration in the Southern Ocean, *Nature*, 7139, 1070–1074, 2007.
- 465 Boyd, P. W., Jickells, T., Law, C. S., Blain, S., Boyle, E. A., Buesseler, K. O., Coale, K. H., Cullen, J. J., Baar,
466 H. J. W. de, Follows, M., Harvey, M., Lancelot, C., Levasseur, M., Owens, N. P. J., Pollard, R., Rivkin, R.
467 B., Sarmiento, J., Schoemann, V., Smetacek, V., Takeda, S., Tsuda, A., Turner, S. and Watson, A. J.:
468 Mesoscale Iron Enrichment Experiments 1993–2005: Synthesis and Future Directions, *Science*, 315,
469 612–617, 2007.
- 470 Buesseler, K. O., Andrews, J. E., Pike, S. M. and Charette, M. A.: The effects of iron fertilization on
471 carbon sequestration in the Southern Ocean, *Science*, 304(5669), 414–417, 2004.
- 472 Bury, S. J., Boyd, P. W., Preston, T., Savidge, G. and Owens, N. J. P.: Size-fractionated primary
473 production and nitrogen uptake during a North Atlantic phytoplankton bloom : implications for
474 carbon export estimates, *Deep Sea Res. Part 1 Oceanogr. Res. Pap.*, 48(3), 689–720; 7, 2001.
- 475 Casacuberta, N., Masqué, P., Henderson, G., Rutgers van-der-Loeff, M., Bauch, D., Vockenhuber, C.,
476 Daraoui, A., Walther, C., Synal, H.-A. and Christl, M.: First 236U data from the Arctic Ocean and use
477 of 236U/238U and 129I/236U as a new dual tracer, *Earth Planet. Sci. Lett.*, 440, 127–134,
478 doi:10.1016/j.epsl.2016.02.020, 2016.
- 479 Castrillejo, M., Casacuberta, N., Christl, M., Vockenhuber, C., Synal, H.-A., García-Ibáñez, M. I.,
480 Lherminier, P., Sarthou, G., García-Orellana, J. and Masqué, P.: Tracing water masses with ¹²⁹I and
481 ²³⁶U in the subpolar North Atlantic along the GEOTRACES GA01 section, *Biogeosciences Discuss.*, 1–
482 28, doi:<https://doi.org/10.5194/bg-2018-228>, 2018.
- 483 Chase, Z., Johnson, K. S., Elrod, V. A., Plant, J. N., Fitzwater, S. E., Pickella, L. and Sakamoto, C. M.:
484 Manganese and iron distributions off central California influenced by upwelling and shelf width, *Mar*
485 *Chem*, 95, 235–254, 2005.
- 486 Copard, K., Colin, C., Frank, N., Jeandel, C., Montero-Serrano, J. C., Reverdin, G. and Ferron, B.: Nd
487 isotopic composition of water masses and dilution of the Mediterranean outflow along the southwest
488 European margin, *Geochem Geophys Geosyst*, 12, Q06020, 10.1029/2011GC003529, 2011.



- 489 Cossa, D., Heimbürger, L.-E., Pérez, F. F., García-Ibáñez, M. I., Sonke, J. E., Planquette, H., Lherminier,
490 P., Boutorh, J., Cheize, M., Menzel Barraqueta, J. L., Shelley, R. and Sarthou, G.: Mercury distribution
491 and transport in the North Atlantic Ocean along the GEOTRACES-GA01 transect, *Biogeosciences*,
492 15(8), 2309–2323, doi:10.5194/bg-15-2309-2018, 2018a.
- 493 Cossa, D., Heimbürger, L. E., Sonke, J. E., Planquette, H., Lherminier, P., García-Ibáñez, M. I., Pérez, F.
494 F. and Sarthou, G.: Sources, cycling and transfer of mercury in the Labrador Sea (Geotraces-Geovide
495 cruise), *Mar. Chem.*, 198, 64–69, doi:10.1016/j.marchem.2017.11.006, 2018b.
- 496 Danialt, N., Mercier, H., Lherminier, P., Sarafanov, A., Falina, A., Zunino, P., Pérez, F. F., Ríos, A. F.,
497 Ferron, B., Huck, T., Thierry, V. and Gladyshev, S.: The northern North Atlantic Ocean mean circulation
498 in the early 21st century, *Prog. Oceanogr.*, 146, 142–158, doi:10.1016/j.pocean.2016.06.007, 2016.
- 499 De La Rocha, C. L., Hutchins, D. A., Brzezinski, M. A. and Zhang, Y.: Effects of iron and zinc deficiency
500 on elemental composition and silica production by diatoms, *Mar Ecol Progr Ser*, 195, 71–79, 2000.
- 501 De La Rocha, C. L., Bescont, P., Croguennoc, A. and Ponzevera, E.: The silicon isotopic composition of
502 surface waters of the Atlantic and Indian sectors of the Southern Ocean, *Geochim. Cosmochim. Acta*,
503 75, 5283–5295, 2011.
- 504 Dehairs, F., Shopova, D., Ober, S., Veth, C. and Goeyens, L.: Particulate barium stocks and oxygen
505 consumption in the Southern Ocean mesopelagic water column during spring and early summer:
506 relationship with export production, *Deep Sea Res. Part II Top. Stud. Oceanogr.*, 44(1), 497–516,
507 doi:10.1016/S0967-0645(96)00072-0, 1997.
- 508 Deng, F., Henderson, G. M., Castrillejo, M. and Perez, F. F.: Evolution of ²³¹Pa and ²³⁰Th in overflow
509 waters of the North Atlantic, *Biogeosciences Discuss*, 2018, 1–24, doi:10.5194/bg-2018-191, 2018.
- 510 Duce, R. A., LaRoche, J., Altieri, K., Arrigo, K. R., Baker, A. R., Capone, D. G., Cornell, S., Dentener, F.,
511 Galloway, J., Ganeshram, R. S., Geider, R. J., Jickells, T., Kuypers, M. M., Langlois, R., Liss, P. S., Liu, S.
512 M., Middelburg, J. J., Moore, C. M., Nickovic, S., Oschlies, A., Pedersen, T., Prospero, J., Schlitzer, R.,
513 Seitzinger, S., Sorensen, L. L., Uematsu, M., Ulloa, O., Voss, M., Ward, B. and Zamora, L.: Impacts of
514 atmospheric anthropogenic nitrogen on the open ocean, *Science*, 320(5878), 893–897,
515 doi:10.1126/science.1150369, 2008.
- 516 Filipova, A., Frank, M., Kienast, M., Rickli, J., Hathorne, E., Yashayaev, I. M. and Pahnke, K.: Water
517 mass circulation and weathering inputs in the Labrador Sea based on coupled Hf–Nd isotope
518 compositions and rare earth element distributions, *Geochim. Cosmochim. Acta*, 199, 164–184,
519 doi:10.1016/j.gca.2016.11.024, 2017.
- 520 Fischer, J., Visbeck, M., Zantopp, R., Nunes, N. and doi.: Interannual to decadal variability of outflow
521 from the Labrador Sea, *Geophys Res Lett*, 37, L24610, doi:10.1029/2010GL045321, 2010.
- 522 Fonseca-Batista, Li, X., Riou, V., Michotey, V., Fripiat, F., Deman, F., Guasco, S., Brion, N., Lemaitre, N.,
523 Planchon, F., Tonnard, M., Planquette, H., Sarthou, G., Elskens, M., Chou, L. and Dehairs, F.: Evidence
524 of high N₂ fixation rates in productive waters of the temperate Northeast Atlantic, *Biogeosciences*
525 Discuss, <https://doi.org/10.5194/bg-2018-220>, in review, 2018.
- 526 Fripiat, F., Cavagna, A.-J., Nicolas, S., Dehairs, F., Andre, L. and Cardinal, D.: Isotopic constraints on the
527 Si-biogeochemical cycle of the Antarctic Zone in the Kerguelen area (KEOPS), *Mar Chem*, 123(1–4),
528 11–22, DOI: 10.1016/j.marchem.2010.08.005, 2011.
- 529 Fröb, F., Olsen, A., Pérez, F. F., García-Ibáñez, M. I., Jeansson, E., Omar, A. and Lauvset, S. K.: Inorganic
530 carbon and water masses in the Irminger Sea since 1991, *Biogeosciences*, 15(1), 51–72,
531 doi:10.5194/bg-15-51-2018, 2018.
- 532 García-Ibáñez, M. I., Pérez, F. F., Lherminier, P., Zunino, P., Mercier, H. and Tréguer, P.: Water mass
533 distributions and transports for the 2014 GEOVIDE cruise in the North Atlantic, *Biogeosciences*, 15(7),
534 2075–2090, doi:10.5194/bg-15-2075-2018, 2018.
- 535 Gourain, A., Planquette, H., Cheize, M., Lemaitre, N., Menzel Barraqueta, J.-L., Shelley, R., Lherminier,
536 P. and Sarthou, G.: Inputs and processes affecting the distribution of particulate iron in the North
537 Atlantic along the GEOVIDE (GEOTRACES GA01) section, *Biogeosciences Discuss*, 2018, 1–42,
538 doi:10.5194/bg-2018-234, 2018.
- 539 Hayes, C. T., Anderson, R. F., Fleisher, M. Q., Huang, K.-F., Robinson, L. F., Lu, Y., Cheng, H., Edwards,
540 R. L. and Moran, S. B.: ²³⁰Th and ²³¹Pa on GEOTRACES GA03, the U.S. GEOTRACES North Atlantic



- 541 transect, and implications for modern and paleoceanographic chemical fluxes, *Deep Sea Res. Part II*
542 *Top. Stud. Oceanogr.*, 116, 29–41, doi:10.1016/j.dsr2.2014.07.007, 2015.
- 543 Henderson, G. M.: New oceanic proxies for paleoclimate, *Earth Planet Sci Lett*, 203, 1–13, 2002.
- 544 Henson, S. A., Dunne, J. P. and Sarmiento, J. L.: Decadal variability in North Atlantic phytoplankton
545 blooms, *J Geophys Res*, 114, C04013, doi:10.1029/2008JC005139, 2009.
- 546 Hsieh, Y.-T., Henderson, G. M. and Thomas, A. L.: Combining seawater ²³²Th and ²³⁰Th concentrations
547 to determine dust fluxes to the surface ocean, *Earth Planet Sci. Lett*, 312, 280–290,
548 doi:10.1016/j.epsl.2011.10.022, 2011.
- 549 Jeandel, C. and Oelkers, E. H.: The influence of terrigenous particulate material dissolution on ocean
550 chemistry and global element cycles, *Chem. Geol.*, 395, 50–66, doi:10.1016/j.chemgeo.2014.12.001,
551 2015.
- 552 Jeandel, C., Peucker Ehrenbrink, B., Jones, M., Pearce, C., Oelkers, E., Godderis, Y., Lacan, F., Aumont,
553 O. and Arsouze, T.: Ocean margins: the missing term for oceanic element budgets?, *EOS*, 92, 217–
554 219, 2011.
- 555 Jickells, T. D., An, Z. S., Andersen, K. K., Baker, A. R., Bergametti, G., Brooks, N., Cao, J. J., Boyd, P. W.,
556 Duce, R. A., Hunter, K. A., Kawahata, H., Kubilay, N., La Roche, J., Liss, P. S., Mahowald, N., Prospero,
557 J. M., Ridgwell, A. J., Tegen, I. and Torres, R.: Global Iron Connections Between Desert Dust, Ocean
558 Biogeochemistry, and Climate, *Science*, 308, 67–71, 2005.
- 559 Kanzow, T., Cunningham, S. A., Johns, W. E., Hirschi, J. J.-M., Marotzke, J., Baringer, M. O., Meinen, C.
560 S., Chidichimo, M. P., Atkinson, C., Beal, L. M., Bryden, H. L. and Collins, J.: Seasonal Variability of the
561 Atlantic Meridional Overturning Circulation at 26.5°N, *J Clim.*, 23, 5678–5698,
562 doi:10.1175/2010JCLI3389.1, 2010.
- 563 Keigwin, L. D. and Boyle, E. A.: Did North Atlantic overturning halt 17,000 years ago?,
564 *Paleoceanography*, 23(1), doi:10.1029/2007PA001500, 2008.
- 565 Key, R. M., Kozyr, A., Sabine, C. L., Lee, K., Wanninkhof, R., Bullister, J. L., Feely, R. A., Millero, F. J.,
566 Mordy, C. and Peng, T.-H.: A global ocean carbon climatology: Results from the Global Data Analysis
567 Project (GLODAP), *Glob. Biogeochem Cycles*, 18, 10.1029/2004GB002247, 2004.
- 568 Lacan, F. and Jeandel, C.: Tracing Papua New Guinea imprint on the central Equatorial Pacific Ocean
569 using neodymium isotopic compositions and Rare Earth Element patterns, *Earth Planet Sci Lett*, 5779,
570 1–16, 2001.
- 571 Lacan, F. and Jeandel, C.: Subpolar Mode Water formation traced by neodymium isotopic composition,
572 *Geophys. Res. Lett.*, 31, L14306, doi:10.1029/2004GL019747, 2004, 2004.
- 573 Lacan, F. and Jeandel, C.: Neodymium isotopes as a new tool for quantifying exchange fluxes at the
574 continent-ocean interface, *Earth Planet Sci Lett*, 232(3–4), 245–257, doi:10.1016/j.epsl.2005.01.004,
575 2005.
- 576 Lambelet, M., van de Flierdt, T., Crockett, K., Rehkämper, M., Kreissig, K., Coles, B., Rijkenberg, M. J. A.,
577 Gerringa, L. J. A., de Baar, H. J. W. and Steinfeldt, R.: Neodymium isotopic composition and
578 concentration in the western North Atlantic Ocean: Results from the GEOTRACES GA02 section,
579 *Geochim. Cosmochim. Acta*, 177(Supplement C), 1–29, doi:10.1016/j.gca.2015.12.019, 2016.
- 580 Lampitt, R. S.: Evidence for the seasonal deposition of detritus to the deep-sea floor and its subsequent
581 resuspension, *Deep Sea Res I*, 32(8), 885–897, 1985.
- 582 Le Reste, S., Dutreuil, V., André, X., Thierry, V., Renaut, C., Le Traon, P.-Y. and Maze, G.: “Deep-Arvor”:
583 A New Profiling Float to Extend the Argo Observations Down to 4000-m Depth, *J. Atmospheric Ocean.*
584 *Technol.*, 33(5), 1039–1055, doi:10.1175/JTECH-D-15-0214.1, 2016.
- 585 Le Roy, E., Sanial, V., Charette, M. A., van Beek, P., Lacan, F., Jacquet, S. H. M., Henderson, P. B.,
586 Souhaut, M., García-Ibáñez, M. I., Jeandel, C., Pérez, F. F. and Sarthou, G.: The ²²⁶Ra-Ba relationship
587 in the North Atlantic during GEOTRACES-GA01, *Biogeosciences Discuss*, 2017, 1–36, doi:10.5194/bg-
588 2017-478, 2017.
- 589 de Leeuw, G., Guieu, C., Arneth, A., Bellouin, N., Bopp, L., Boyd, P. W., Denier van der Gon, H. A. C.,
590 Desboeufs, K. V., Dulac, F., Facchini, M. C., Gantt, B., Langmann, B., Mahowald, N. M., Marañón, E.,
591 O’Dowd, C., Olgun, N., Pulido-Villena, E., Rinaldi, M., Stephanou, E. G. and Wagener, T.: Ocean-
592 atmosphere interactions of particles, in *Ocean-Atmosphere Interactions of Gases and Particles*,



- 593 edited by M. T. Johnson, p. 171–246, DOI 10.1007/978–3–642–25643–1_4, Springer: Heidelberg,
594 2014.
- 595 Lemaitre, N., Planchon, F., Planquette, H., Dehairs, F., Fonseca-Batista, D., Roukaerts, A., Deman, F.,
596 Tang, Y., Mariez, C. and Sarthou, G.: High variability of export fluxes along the North Atlantic
597 GEOTRACES section GA01: Particulate organic carbon export deduced from the 234Th method,
598 Biogeosciences Discuss, 2018, 1–38, doi:10.5194/bg-2018-190, 2018a.
- 599 Lemaitre, N., Planquette, H., Planchon, F., Sarthou, G., Jacquet, S., García-Ibáñez, M. I., Gourain, A.,
600 Cheize, M., Monin, L., André, L., Laha, P., Terryn, H. and Dehairs, F.: Particulate barium tracing of
601 significant mesopelagic carbon remineralisation in the North Atlantic, Biogeosciences, 15(8), 2289–
602 2307, doi:10.5194/bg-15-2289-2018, 2018b.
- 603 Lherminier, P., Mercier, H., Huck, T., Gourcuff, C., Perez, F. F., Morin, P. and Sarafanov, A.: The Atlantic
604 meridional overturning circulation and the subpolar gyre observed at the A25-Ovide section in June
605 2002 and 2004, Deep Sea Res I, 57(11), 1374–1391, doi:10.1016/j.dsr.2010.07.009, 2010.
- 606 Mahowald, N. M., Baker, A. R., Bergametti, G., Brooks, N., Duce, R. A., Jickells, T. D., Kubilay, N.,
607 Prospero, J. M. and Tegen, I.: Atmospheric global dust cycle and iron inputs to the ocean, Glob.
608 Biogeochem Cy, 19, GB4025, doi:10.1029/2004GB002402., 2005.
- 609 McManus, J. F., Francois, R., Gherardi, J.-M., Keigwin, L. D. and Brown-Leger, S.: Collapse and rapid
610 resumption of Atlantic meridional circulation linked to deglacial climate changes, Nature, 428, 834–
611 837, 2004.
- 612 Measures, C. I. and Brown, E. T.: Estimating dust input to the Atlantic Ocean using surface water Al
613 concentrations, in The impact of African Dust across the Mediterranean, edited by Guerzoni and
614 Chester, p. 389, Kluwer., 1996.
- 615 Menzel Barraqueta, Klar, J.K., Gledhill, M., Schlosser, C., Shelley, R., Wenzel, B., Sarthou, G. and
616 Achterberg, E.: Atmospheric aerosol deposition fluxes over the Atlantic Ocean: A GEOTRACES case
617 study, Biogeosciences Discuss, 2018a.
- 618 Menzel Barraqueta, J.-L., Schlosser, C., Planquette, H., Gourain, A., Cheize, M., Boutorh, J., Shelley, R.,
619 Pereira Contreira, L., Gledhill, M., Hopwood, M. J., Lherminier, P., Sarthou, G. and Achterberg, E. P.:
620 Aluminium in the North Atlantic Ocean and the Labrador Sea (GEOTRACES GA01 section): roles of
621 continental inputs and biogenic particle removal, Biogeosciences Discuss, 2018, 1–28,
622 doi:10.5194/bg-2018-39, 2018b.
- 623 Mercier, H., Lherminier, P., Sarafanov, A., Gaillard, F., Daniault, N., Desbruyères, D., Falina, A., Ferron,
624 B., Gourcuff, C., Huck, T. and Thierry, V.: Variability of the Meridional Overturning Circulation at the
625 Greenland-Portugal Ovide section from 1993 to 2010, Prog. Oceanogr., 132, 250–261,
626 <http://dx.doi.org/10.1016/j.pocean.2013.11.001>, 2015.
- 627 Montero-Serrano, J. C., Frank, N., Tisnérat-Laborde, N., Colin, C., Wu, C. C., Lin, K., Shen, C. C., Copard,
628 K., Orejas, C., Gori, A., De Mol, L., Van Rooij, D., Reverdin, G. and Douville, E.: Decadal changes in the
629 mid-depth water mass dynamic of the Northeastern Atlantic margin (Bay of Biscay), Earth Planet Sci
630 Lett, 364, 134–144, 2013.
- 631 Moran, S. B., Shen, C.-C., Edmonds, H. N., Weinstein, S. E., Smith, J. N. and Edwards, R. L.: Dissolved
632 and particulate 231Pa and 230Th in the Atlantic Ocean: constraints on intermediate/deep water age,
633 boundary scavenging, and 231Pa/230Th fractionation, Earth Planet Sci Lett, 203(3–4), 999–1014,
634 doi:10.1016/S0012-821X(02)00928-7, 2002.
- 635 Negre, C., Zahn, R., Thomas, A. L., Masque, P., Henderson, G. M., Martinez-Mendez, G., Hall, I. R. and
636 Mas, J. L.: Reversed flow of Atlantic deep water during the Last Glacial Maximum, Nature, 468, 84–
637 88, 2010.
- 638 Pérez, F. F., Mercier, H., Vázquez-Rodríguez, M., Lherminier, P., Velo, A., Pardo, P. C., Rosón, G. and
639 Ríos, A. F.: Atlantic Ocean CO₂ uptake reduced by weakening of the meridional overturning
640 circulation, Nat. Biogeoscience, doi: 10.1038/NNGEO1680, 2013.
- 641 Perez, F. F., Fontela, M., García-Ibáñez, M. I., Mercier, H., Velo, A., Lherminier, P., Zunino, P., Paz, M.
642 de la, Alonso-Pérez, F., Guallart, E. F. and Padin, X. A.: Meridional overturning circulation conveys fast
643 acidification to the deep Atlantic Ocean, Nature, 554(7693), 515–518, doi:10.1038/nature25493,
644 2018.



- 645 Pollard, R., Sanders, R., Lucasa, M. and Statham, P.: The Crozet Natural Iron Bloom and Export
646 Experiment (CROZEX), *Deep Sea Res II*, 54(18–20), 1905–1914, 2007.
- 647 Reverdin, G., Cayan, D., Dooley, H. D., Ellett, D. J., Levitus, S., Du Penhoat, Y. and Dessier, A.: Surface
648 salinity of the North Atlantic: Can we reconstruct its fluctuations over the last one hundred years?,
649 *Progr Ocean.*, 33, 303–346, 1994.
- 650 Roca-Martí, M., Puigcorbé, V., Loeff, M. M. R. van der, Katlein, C., Fernández-Méndez, M., Peeken, I.
651 and Masqué, P.: Carbon export fluxes and export efficiency in the central Arctic during the record
652 sea-ice minimum in 2012: a joint ²³⁴Th/²³⁸U and ²¹⁰Po/²¹⁰Pb study, *J. Geophys. Res. Oceans*,
653 121(7), 5030–5049, doi:10.1002/2016JC011816, 2016.
- 654 Sabine, C. L., Feely, R. A., Gruber, N., Key, R. M., Lee, K., Bullister, J. L., Wanninkhof, R., Wong, C. S.,
655 Wallace, D. W. R., Tilbrook, B., Millero, F. J., Peng, T.-H., Kozyr, A., Ono, T. and Rios, A. F.: The oceanic
656 sink for anthropogenic CO₂, *Science*, 682(305), 367–371, 2004.
- 657 Savidge, G., Boyd, P., Pomroy, A., Harbour, D. and Joint, I.: Phytoplankton production and biomass
658 estimates in the Northeast Atlantic Ocean, May–June 1990, *Deep Sea Res I*, 42(5), 599–617, 1995.
- 659 Schlitzer, R.: Ocean Data View, online: <https://odv.awi.de>, [24 Nov 2017], 2017.
- 660 Seager, R., Battisti, D. S., Yin, J., Gordon, N., Naik, N., Clement, A. C. and Cane, M. A.: Is the Gulf Stream
661 responsible for Europe’s mild winters?, *Q J R Meteorol Soc*, 128(586), 2563–2586, 2002.
- 662 Shelley, R. U., Roca-Martí, M., Castrillejo, M., Sanial, V., Masqué, P., Landing, W. M., van Beek, P.,
663 Planquette, H. and Sarthou, G.: Quantification of trace element atmospheric deposition fluxes to the
664 Atlantic Ocean (>40°N; GEOVIDE, GEOTRACES GA01) during spring 2014, *Deep Sea Res. Part*
665 *Oceanogr. Res. Pap.*, 119, 34–49, doi:10.1016/j.dsr.2016.11.010, 2017.
- 666 Shelley, R. U., Landing, W. M., Ussher, S. J., Planquette, H. and Sarthou, G.: Regional trends in the
667 fractional solubility of Fe and other metals from North Atlantic aerosols (GEOTRACES cruises GA01
668 and GA03) following a two-stage leach, *Biogeosciences*, 15(8), 2271–2288, doi:10.5194/bg-15-2271-
669 2018, 2018.
- 670 Sutton, J. N., de Souza, G. F., García-Ibáñez, M. I. and De La Rocha, C. L.: The silicon stable isotope
671 distribution along the GEOVIDE section of the North Atlantic Ocean, *Biogeosciences Discuss*, 2018,
672 1–28, doi:10.5194/bg-2018-165, 2018.
- 673 Tang, Y., Castrillejo, M., Roca-Martí, M., Masqué, P., Lemaître, N. and Stewart, G.: Distributions of ²¹⁰Po
674 and ²¹⁰Pb activities along the North Atlantic GEOTRACES GA01 (GEOVIDE) cruise: partitioning
675 between the particulate and dissolved phase, *Biogeosciences Discuss.*, 1–34,
676 doi:<https://doi.org/10.5194/bg-2018-210>, 2018.
- 677 Tonnard, M., Planquette, H., Bowie, A. R., van der Merwe, P., Gallinari, M., Desprez de Gésincourt, F.,
678 Germain, Y., Gourain, A., Benetti, M., Reverdin, G., Tréguer, P., Boutorh, J., Cheize, M., Menzel
679 Barraqueta, J.-L., Pereira-Contreira, L., Shelley, R., Lherminier, P. and Sarthou, G.: Dissolved iron in
680 the North Atlantic Ocean and Labrador Sea along the GEOVIDE section (GEOTRACES section GA01),
681 *Biogeosciences Discuss*, 2018, 1–53, doi:10.5194/bg-2018-147, 2018.
- 682 Wischmeyer, A. G., Del Amo, Y., Brzezinski, M. and Wolf-Gladrow, D. A.: Theoretical constraints on the
683 uptake of silicic acid species by marine diatoms, *Mar Chem*, 82(1–2), 13–29, 2003.
- 684 Xu, X., Hulbert, H. E., Schmitz Jr., W. J., Zantopp, R., Fischer, J. and Hogan, J.: On the currents and
685 transports connected with the Atlantic Meridional Overturning Circulation in the subpolar North
686 Atlantic, *J Geophys Res*, in press, doi: 10.1002/jgrc.20065, 2013.
- 687 Zunino, P., Lherminier, P., Mercier, H., Padín, X.A., Ríos, A.F. and Pérez, F.F.: Dissolved inorganic carbon
688 budgets in the eastern subpolar North Atlantic in the 2000s from in situ data, *Geophys. Res. Lett.*,
689 42(22), 9853–9861, doi:10.1002/2015GL066243, 2015.
- 690 Zunino, P., Lherminier, P., Mercier, H., Daniault, N., García-Ibáñez, M. I. and Pérez, F. F.: The GEOVIDE
691 cruise in May–June 2014 reveals an intense Meridional Overturning Circulation over a cold and fresh
692 subpolar North Atlantic, *Biogeosciences*, 14(23), 5323–5342, doi:10.5194/bg-14-5323-2017, 2017.
- 693 Zurbrick, C. M., Boyle, E. A., Kayser, R., Reuer, M. K., Wu, J., Planquette, H., Shelley, R., Boutorh, J.,
694 Cheize, M., Contreira, L., Menzel Barraqueta, J.-L. and Sarthou, G.: Dissolved Pb and Pb isotopes in
695 the North Atlantic from the GEOVIDE transect (GEOTRACES GA-01) and their decadal evolution,
696 *Biogeosciences Discuss*, 2018, 1–34, doi:10.5194/bg-2018-29, 2018.



697 **Figure captions**

698 **Figure 1:** Schematic diagram of the mean large-scale circulation adapted from Danialt et al.
699 (2016) and Zunino et al. (2017). Bathymetry is plotted in color with color changes at 100 and
700 1000m and every 1000m below 1000 m. Black dots represent the Short station, yellow stars
701 the Large ones, orange stars the XLarge ones, and red stars the Super ones. The main water
702 masses are indicated: Denmark Strait Overflow Water (DSOW), Iceland–Scotland Overflow
703 Water (ISOW), Labrador Sea Water (LSW), Mediterranean Water (MW), and lower Northeast
704 Atlantic Deep Water (LNEADW).

705 **Figure 2:** Section plots for (a) salinity, (b) potential temperature ($^{\circ}\text{C}$), (c) dissolved oxygen
706 ($\mu\text{mol kg}^{-1}$), (d) nitrate + nitrite ($\mu\text{mol L}^{-1}$), and (e) silicic acid ($\mu\text{mol L}^{-1}$) during the GEOVIDE
707 cruise. Water masses are indicated in black, MW: Mediterranean Water; ENACW: North
708 Atlantic Central Water; NEADW: North East Atlantic Deep Water; LSW: Labrador Sea Water;
709 ISOW: Iceland-Scotland Overflow Water; SAIW: Sub-Arctic Intermediate Water; IcSPMW:
710 Iceland Sub-Polar Mode Water; IrSPMW: Irminger Sub-Polar Mode Water. Station locations
711 are indicated by the numbers on top of the panel. These plots were generated by Ocean Data
712 View (Schlitzer, 2017).

713 **Figure 3:** Section plots for (a) biogenic silica (BSi, $\mu\text{mol L}^{-1}$), (b) particulate organic carbon (POC,
714 $\mu\text{mol L}^{-1}$), and (c) particulate organic nitrogen (PON, $\mu\text{mol L}^{-1}$), during the GEOVIDE cruise.
715 Station locations are indicated by the numbers on top of the panel. These plots were
716 generated by Ocean Data View (Schlitzer, 2017).

717

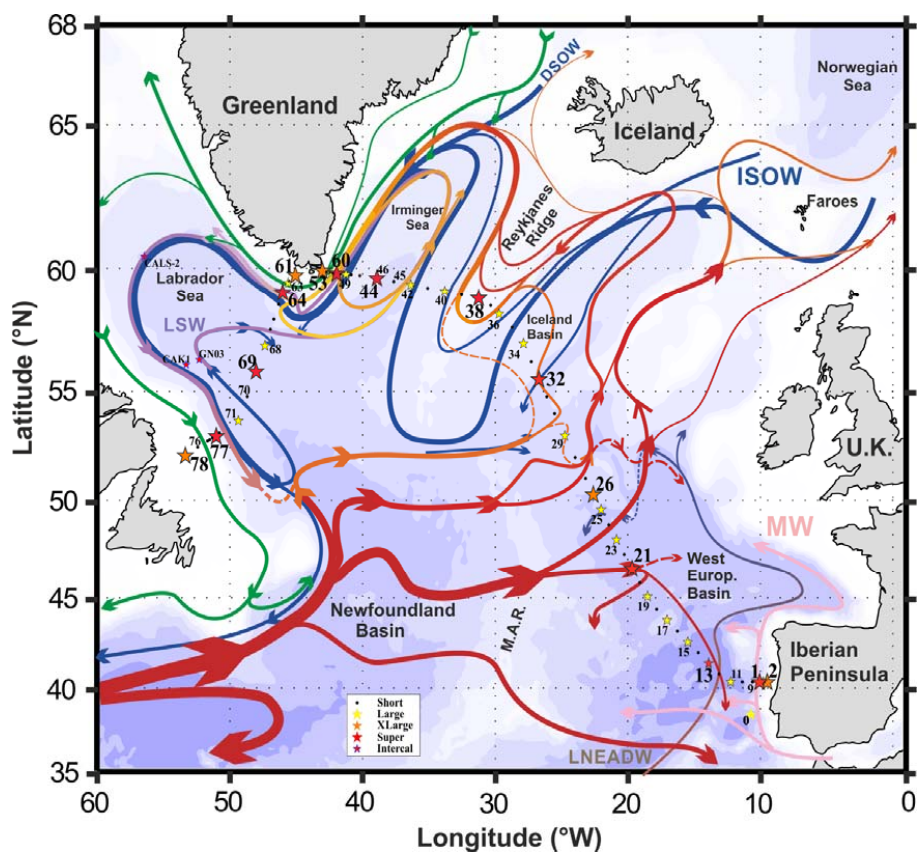
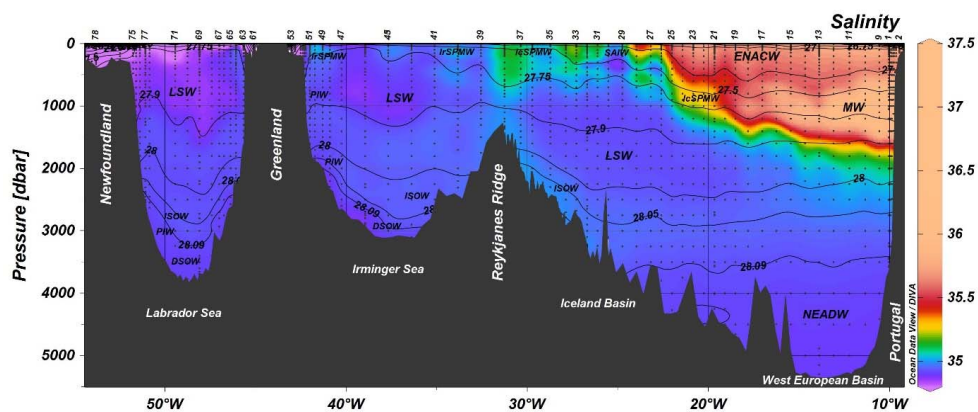
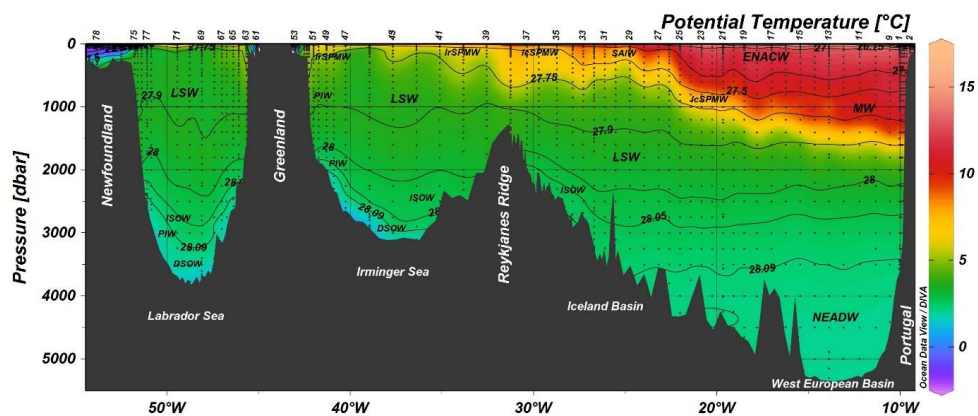


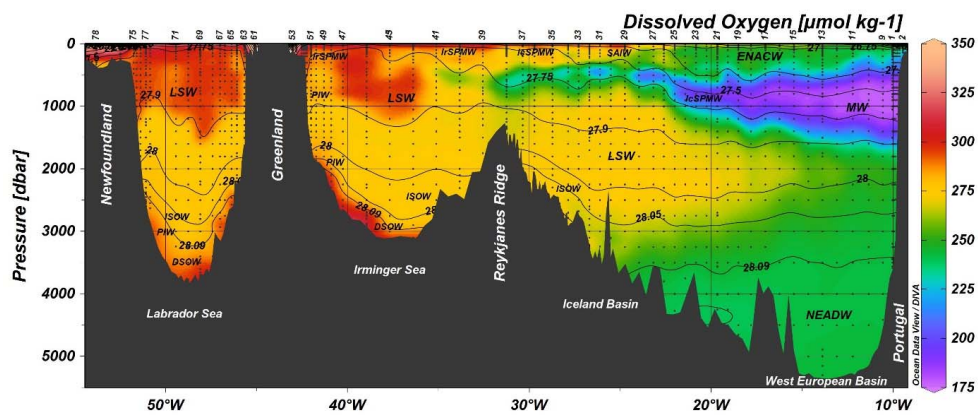
Figure 1



(a)



(b)



(c)

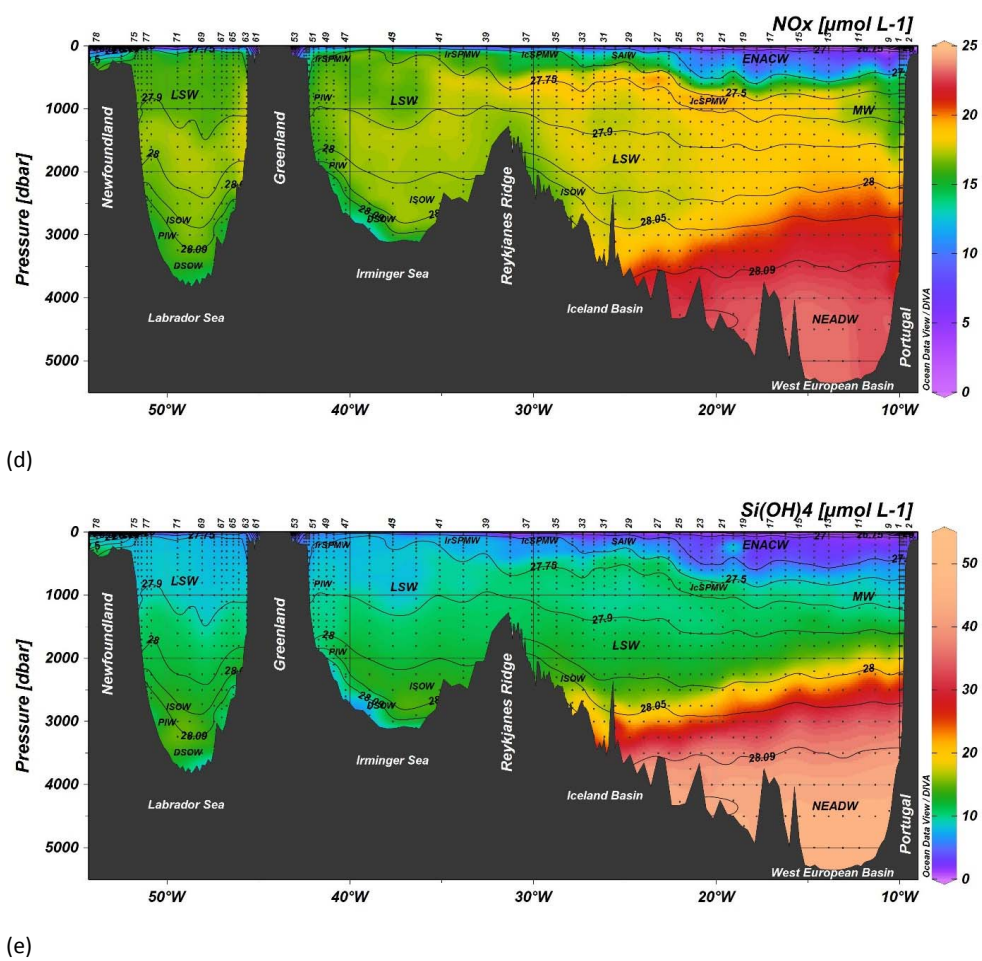


Figure 2

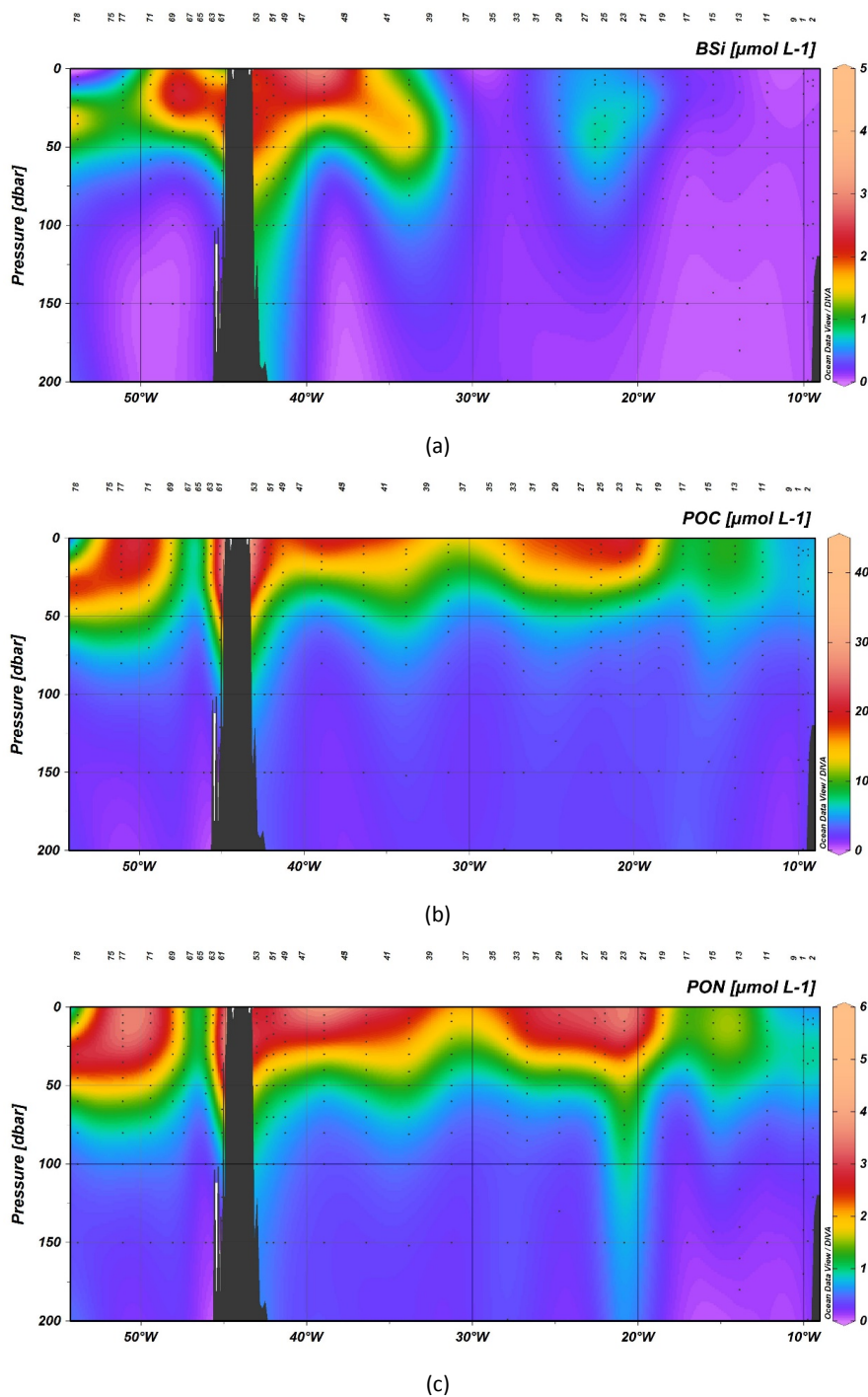


Figure 3